Phosphatidylinositol-4-phosphate-dependent membrane traffic is critical for fungal filamentous growth

Vikram Ghugtyal[a,b,c], Rocio Garcia-Rodas[a,b,c], Agnese Seminara[d], Sébastien Schaub[a,b,c], Martine Bassilana[a,b,c], and Robert Alan Arkowitz[a,b,c,1]

[a]Université de Nice-Sophia Antipolis, Institute of Biology Valrose, Parc Valrose, 06108 Nice Cedex 2, France; [b]CNRS Institute of Biology Valrose, UMR7277, Parc Valrose, 06108 Nice Cedex 2, France; [c]INSERM Institute of Biology Valrose, UMR1091, Parc Valrose, 06108 Nice Cedex 2, France; and [d]CNRS, Université de Nice-Sophia Antipolis, Laboratoire de Physique de la Matière Condensée-UMR 7336, Avenue J. Vallot, 06108 Nice Cedex 2, France

Edited by William T. Wickner, Geisel School of Medicine at Dartmouth College, Hanover, NH, and approved June 1, 2015 (received for review March 2, 2015)

The phospholipid phosphatidylinositol-4-phosphate [PI(4)P], generated at the Golgi and plasma membrane, has been implicated in many processes, including membrane traffic, yet its role in cell morphology changes, such as the budding to filamentous growth transition, is unknown. We show that Golgi PI(4)P is required for such a transition in the human pathogenic fungus *Candida albicans*. Quantitative analyses of membrane traffic revealed that PI(4)P is required for late Golgi and secretory vesicle dynamics and targeting and, as a result, is important for the distribution of a multidrug transporter and hence sensitivity to antifungal drugs. We also observed that plasma membrane PI(4)P, which we show is functionally distinct from Golgi PI(4)P, forms a steep gradient concomitant with filamentous growth, despite uniform plasma membrane PI-4-kinase distribution. Mathematical modeling indicates that local PI(4)P generation and hydrolysis by phosphatases are crucial for this gradient. We conclude that PI(4)P-regulated membrane dynamics are critical for morphology changes.

membrane traffic | filamentous growth | polarity | morphogenesis | lipid distribution

Phosphatidylinositol-4-phosphate [PI(4)P] is a minor constituent of cellular membranes that is essential for polarized growth, membrane traffic, and cytoskeleton organization (1–3). The majority of PI(4)P in budding yeast is generated by two essential PI-4-kinases, Pik1 at the Golgi and Stt4 at the plasma membrane (PM) (4–7). Although we have shown that PM Stt4 and the PI(4)P-5-kinase Mss4 are critical for the human fungal pathogen *Candida albicans* filamentous growth (8), little is known regarding the importance of Golgi PI(4)P. Perturbation of Golgi PI(4)P levels in *Saccharomyces cerevisiae* and mammalian cells results in defects in Golgi morphology and secretion (9–13). Furthermore, the Golgi in mammalian cells is important for cell polarity (14). In the filamentous fungus *Neurospora crassa*, PI(4)P has been observed at the Golgi (15), yet its function is unknown.

In a range of fungi, including pathogenic species, a morphological transition between yeast and filamentous forms, triggered by numerous external stimuli, is important for virulence (16, 17). Many proteins localize to the tip of the *C. albicans* protruding filament and a number of proteins are either secreted or incorporated into the cell wall during the yeast to filamentous morphological transition (17), alluding to the importance of membrane traffic in this process. Here we show that cells with reduced Golgi PI(4)P levels are defective in morphogenesis and that Golgi PI(4)P is critical for two distinct steps in the secretory pathway. Furthermore, we observed a striking gradient of PM PI(4)P along the length of the hyphal filament and mathematical modeling revealed the processes crucial for this distribution.

Results

Golgi PI(4)P Is Critical for Invasive Filamentous Growth. As the *PIK1* gene is located in the mating-type locus (MTL), the two copies are nonidentical, encoding proteins 57% identical. When either *PIK1a* or *PIK1α* was deleted, cells were viable and undergo invasive filamentous growth (Fig. 1 *A* and *B*). However, we were unable to delete both *PIK1* genes and when the remaining copy was placed behind the Tet promoter (Fig. S1 *A* and *B*), cells were inviable upon full repression with doxycycline (Dox) (Fig. 1*A*). Intermediate repression conditions were identified in which both strains were viable (Fig. 1*A*). In the absence of Dox, the *pik1aΔ*/*pTetPIK1α* strain had higher levels of *PIK1α* mRNA than the wild type (WT); upon partial repression these levels were substantially reduced and similar to that of a WT strain (Fig. S1*C*). Both *pik1* mutants had a normal morphology (Fig. 1*C*), yet grew with a $t_{doubling}$ 90% longer than the WT strain, upon partial repression. These partial repression conditions were used hereafter to examine the role of *PIK1* in filamentous growth.

In the presence of FCS without repression (−Dox), filamentous growth of these *pik1* mutants was similar to that of the WT (Fig. 1 *B* and *C*). In contrast, upon *PIK1* repression (+Dox) we observed striking defects in filamentous growth, which were rescued by the respective *PIK1* copy (Fig. 1 *B* and *C*). Nonetheless, the *pik1aΔ*/*pTetPIK1α* strain (hereafter referred to as *pik1*) still responded to FCS, as induction of hyphal specific genes was observed, albeit to 5- to 10-fold lower levels (Fig. S1*D*). With respect to viability, ∼10% of *pik1* mutant cells were inviable upon *PIK1* repression (Fig. S1*F*), similar to *stt4* and *mss4* mutants (8). Also, just as addition of the osmo-support sorbitol improved the growth of *S. cerevisiae pik1*^{ts} (7, 10) and *C. albicans stt4* and *mss4* mutants (8), sorbitol reduced the *pik1* mutant inviability (Fig. S1*F*), yet did not alter the filamentous growth defect. Together, our results show that Pik1 is necessary for filamentous growth.

Significance

Cell morphology changes in response to external stimuli require both identification of a growth site and concomitant membrane traffic directed to this site. We have previously shown that plasma membrane phosphatidylinositol-bis-phosphate PI(4,5)P_2 is critical for fungal filamentous growth. Here we show that the Golgi phosphatidylinositol-4-phosphate [PI(4)P] is essential for the yeast to filamentous growth transition, via its role in Golgi function and dynamics. Furthermore, we have modeled the steep gradient of this lipid at the plasma membrane and propose that local generation, as well as hydrolysis by phosphatases, is critical. Our results demonstrate that PI(4)P-regulated membrane dynamics are key for cell morphology changes.

Author contributions: M.B. and R.A.A. designed research; V.G., R.G.-R., A.S., and R.A.A. performed research; V.G., A.S., S.S., and R.A.A. contributed new reagents/analytic tools; V.G., R.G.-R., A.S., S.S., M.B., and R.A.A. analyzed data; and R.A.A. wrote the paper.

The authors declare no conflict of interest.

This article is a PNAS Direct Submission.

[1]To whom correspondence should be addressed. Email: arkowitz@unice.fr.

This article contains supporting information online at www.pnas.org/lookup/suppl/doi:10.1073/pnas.1504259112/-/DCSupplemental.

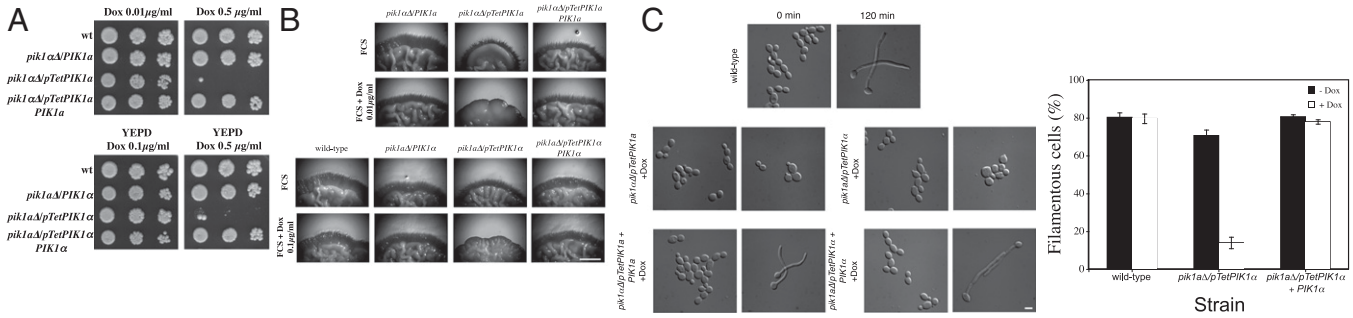

Fig. 1. Pik1 is required for invasive filamentous growth. (*A*) Strains with partial repression of *PIK1* are viable. Indicated strains were incubated with or without Dox on rich media containing agar for 5 d. (*B*) Strains with partial repression of *PIK1* are defective in invasive filamentous growth. Indicated strains were incubated on FCS containing agar with or without Dox for 5 d. (*C*) Pik1 is necessary for hyphal growth. Indicated strains were grown in the presence (0.01 μg/mL for *pik1αΔ/pTetPIK1a* strains and 0.1 μg/mL for *pik1aΔ/pTetPIK1α* strains) of Dox with or without FCS. In the absence of Dox all strains formed hyphae. Filamentous cells (%) were determined from three experiments, $n = 80$ cells; SD shown.

Little to no perturbation of the actin cytoskeleton was observed in the *C. albicans pik1* mutants (Fig. S2 *A* and *B*), in contrast to some *S. cerevisiae pik1*^{ts} mutants (12). As both Cdc42 and Rho1 are critical for filamentous growth in *C. albicans* and PI(4,5)P_2 is required for active Rho1 polarized distribution (18), we examined whether Pik1 was important for the localization of these active GTPases. These active GTPases localized similarly in *pik1* and WT cells, with only ∼20% decrease in cells with a polarized distribution in the mutant (Fig. S2 *C* and *D*). As the exocyst subunit Sec3 binds PI(4,5)P_2 in *S. cerevisiae* (19), we also examined whether its location was altered in the *pik1* mutant. Although there was increased Sec3-GFP cytoplasmic signal upon *PIK1* repression, Sec3 localized to growth sites in the majority of the cells (Fig. S2 *E* and *F*). Together, these results indicate that the *pik1* filamentous growth defect is not due to actin cytoskeleton perturbation or an altered localization of active Cdc42, Rho1, or Sec3.

Golgi PI(4)P Is Required for Membrane Traffic. As Pik1 is critical for membrane traffic in *S. cerevisiae* (5, 9–12, 20–22), we investigated whether the impaired yeast to filamentous growth transition in the *pik1* mutant was due to a defect in this process. We first examined the distribution of the multidrug ABC transporter Cdr1 (23), critical for resistance to antifungal drugs (24). This transporter was found exclusively at the PM in WT and *pik1* cells grown in the absence of Dox (Fig. 2*A*). However, upon *PIK1* repression, we observed a majority of cells with intracellular Cdr1-GFP, even though PM Cdr1-GFP was still observed (Fig. 2*A*). Consistent with a defect in Cdr1 PM targeting, the *pik1* mutant specifically exhibited increased drug sensitivity (Fig. 2*B* and Fig. S3*A*). However, the secretion of GFP, fused to the signal sequence of the hyphal cell wall protein Hwp1, was identical in *pik1* and WT strains, indicating that although the distribution of membrane proteins is altered upon *PIK1* repression, protein secretion is largely unaffected, in contrast to *S. cerevisiae* (9, 10, 12). Next, we examined endocytosis using the membrane dye FM4-64. Although we did not detect a defect in PM uptake upon *PIK1* repression, there was a substantial delay in FM4-64 arrival to the vacuole, with the $t_{1/2}$ for vacuole accumulation increased fivefold (Fig. 2*C* and Fig. S3*B*). As FM4-64 colocalized with the late Golgi reporter Sec7-GFP in WT cells (Fig. S3*C*), we attribute this defect to perturbation of the Golgi. Together these results show that Pik1, and hence Golgi PI(4)P, is important for distinct membrane traffic steps.

As PI(4)P has been shown to control recruitment of the Sec4 Rab GEF Sec2 to secretory vesicles (SVs) (22) and also to be critical for myosin-V Myo2-dependent secretion in *S. cerevisiae* (11), we examined SV distribution and targeting in the *C. albicans pik1* mutant, using GFP-Sec4. Quantification of the total GFP-Sec4 signal in the mother and bud compartments revealed an 80% increase in the mother to bud signal ratio upon *PIK1* repression (Fig. 3*A* and Fig. S3*D*; average mother/bud signal 2.4 ± 0.3 SEM without Dox compared with 4.3 ± 0.7 SEM with Dox; $P < 0.05$); the levels of this reporter were unaffected (Fig. S3*E*). As this accumulation of SVs in the mother cell suggested that Pik1 was required for their targeting to growth sites, we manually tracked SV movement in a single z section over time and observed a significant number of vesicles moving from the mother to bud compartment (Fig. 3*B*); on average 6.3 ± 1.9 SVs crossed the bud neck in a single z section over 75 s in the *pik1* mutant strain in the absence of Dox, similar to the WT strain (Fig. 3*C* and Fig. S3*F*). In contrast, in the *pik1* mutant in the presence of Dox we rarely observed SV movement between these two compartments (Fig. 3*B*), with an ∼10-fold decrease (average of 0.6 ± 1.3 SVs) (Fig. 3*C*). The mean-square displacement (MSD) of SVs in *pik1* cells in the absence of repression was determined using the power function $\mathrm{MSD}(t) = A \cdot t^{\alpha},\ t \in [0, 5]\mathrm{s}$ and separating the tracks based upon the scaling component α into those with confined movement ($\alpha < 0.4$) and those with directed movement ($\alpha > 1.4$). This analysis revealed a small population of SVs that moved in a directed fashion (4% of tracks in the absence or the presence of FCS; Fig. S3*G*). Strikingly, the MSD of SVs in hyphae was approximately twice that of budding cells. Together these results suggest that Golgi PI(4)P levels are critical for SVs trafficking to the growth site during the *C. albicans* bud to hyphal transition.

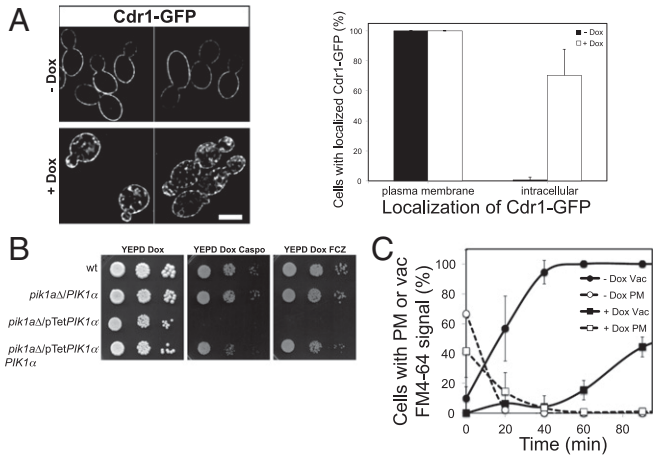

Fig. 2. Pik1 is critical for membrane traffic. (*A*) Pik1 is critical for Cdr1 localization to the PM. (*A*, *Left*) Deconvolved central z section of *pik1* cells expressing Cdr1-GFP. (*A*, *Right*) Percentage of cells with PM and intracellular localized Cdr1-GFP from two experiments, $n = 100$ cells; SD shown. (*B*) The *pik1* mutant is hypersensitive to antifungal drugs. Indicated strains were incubated in the presence of Dox with Caspo at 125 ng/mL and FCZ at 5 μg/mL. (*C*) Pik1 is required for transport of FM4-64 to the vacuole. *Pik1* cells grown with or without Dox were incubated with FM4-64 on ice and uptake was followed over time at 30 °C. Averages (three experiments of $n = 50$ cells) with SD are shown.

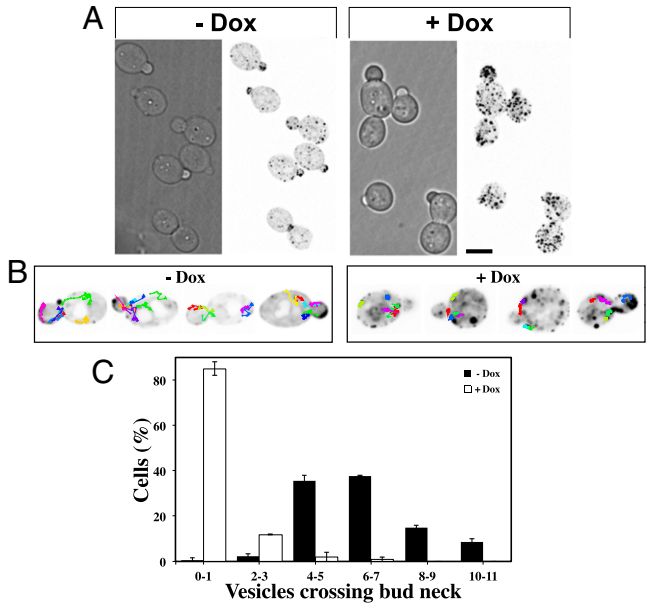

Fig. 3. Pik1 is required for targeting of secretory vesicles. (*A*) Pik1 is required for restricting SVs to sites of growth. Maximum projections of *pik1* cells expressing GFP-Sec4 in the presence and absence of Dox are shown with an inverted look up table (LUT). (*B*) Pik1 is required for targeting of SVs to the bud. Shown are tracks of SV movement from representative *pik1* cells; images were acquired at a single z section every 0.25 s. (*C*) Quantification of SVs crossing the bud neck. Cells as in *B* were imaged over 75 s. Shown is the average number of SVs crossing the bud neck per cell (two experiments of $n = 50$ cells); bars indicate values.

Reduction of Late Golgi PI(4)P Results in Golgi Proliferation and Confined Movement. To further investigate the role of Golgi PI(4)P we examined its distribution, using as a reporter the phosphatidylinositol-4-phosphate adaptor protein-1 (FAPP1) PH domain, which specifically binds this lipid (25). With a *C. albicans* codon-optimized PH^{FAPP1}-GFP reporter, we observed a punctate distribution in WT cells (Fig. S4*A*) characteristic of the Golgi (26) and a decrease in the signal associated with these punctae in the *pik1* mutant upon repression (Fig. S4*A*). As FAPP1 has been shown to also bind Arf1 (27), we mutated the residues responsible for this interaction to make the reporter specific for PI(4)P (28), hereafter referred to as $PI(4)P^{FAPP1}$. Here as well, a punctate distribution was observed in both WT and *pik1* mutant cells, which became substantially fainter upon *PIK1* repression (Fig. S4*B*). The punctae were highly dynamic in WT budding and hyphal cells and appeared to localize preferentially at the filament tip (Fig. S4 *C–E* and Movies S1 and S2), as previously observed with the GDP-mannose transporter Vrg4 (26) and Sec7 (29). In contrast, there was no difference in the signal between bud and mother cell.

To determine the localization of PI(4)P, we used different Golgi markers such as the early Golgi Vrg4 (30) and the late Golgi Sec7 (31), together with Pik1 and Sec4. As Golgi punctae moved rapidly, two-color simultaneous acquisition was carried out with cells expressing these different GFP markers and $PI(4)P^{FAPP1\text{-}mCh}$. In budding and hyphal cells, we detected little colocalization of $PI(4)P^{FAPP1\text{-}mCh}$ with Vrg4-GFP, GFP-Sec4, or the integral Golgi protein Sys1-GFP (Fig. S5 *A–E*). In contrast, substantial colocalization was observed between $PI(4)P^{FAPP1\text{-}mCh}$ and GFP-Pik1 or Sec7-GFP (Fig. S5 *A–C*). With this FAPP1 reporter little to no PI(4)P was observed on SVs, in contrast to *S. cerevisiae* (11, 22).

As our results indicated that PI(4)P is generated by Pik1 at the late Golgi, we examined the PI(4)P levels, the number of Golgi particles, and their dynamics in the *pik1* mutant. Initially, we examined the apparent Golgi PI(4)P concentration by quantifying the mean $PI(4)P^{FAPP1}$ signal per particle surface area. Upon repression of *PIK1*, there was a dramatic decrease in the average concentration of PI(4)P at the Golgi, from 32.3 ± 1.2 SEM without Dox to 5.9 ± 0.2 SEM with Dox (Fig. 4*A* and Fig. S6*A*), compared with WT cells, which were unaffected (Fig. S6*C*). In contrast, the average concentration of Sec7-GFP was unaffected by *PIK1* repression (Fig. 4*A* and Fig. S6*B*). In conjunction with the decreased Golgi PI(4)P levels, there was an increase in the average number of Golgi particles per cell (from 5.5 ± 0.4 SEM to 15.4 ± 1.2 SEM in the absence or presence of Dox, respectively) (Fig. 4*B* and Fig. S6*A*) and again the WT strain was unaffected (Fig. S6*D*). The increase in the number of Golgi particles upon PI(4)P reduction was independently confirmed, as the number of Sec7 punctae per cell also increased (from 10.5 ± 0.4 SEM to 18.6 ± 1.0 SEM) (Fig. 4*B* and Fig. S6*B*), together with the number of Sys1-GFP punctae (from 4.9 ± 0.3 SEM to 20.6 ± 1.6 SEM in the absence or presence of Dox, respectively). These data are consistent with the notion that reduced Golgi PI(4)P results in proliferation of this organelle, further supported by the observation of an ∼1.8-fold increase in the average total Sec7 per cell in the *pik1* mutant in the presence of Dox ($n = 25$ cells; $P < 0.0001$). In *S. cerevisiae* an increase in ring-shaped structures representing exaggerated Golgi membranes was observed in a $pik1^{ts}$ mutant (10). On the other hand, we were unable to detect a change in the Golgi size, inconsistent with organelle fragmentation. We attribute this proliferation to a defect in vesicle budding from the late Golgi. Finally, as Pik1 may be important for gene transcription in *S. cerevisiae* (5), we also verified that the mRNA transcript levels of the analyzed *SEC* and *CDR1* genes were not altered in the *pik1* mutant (Fig. S1*E*).

To determine whether perturbation of Golgi PI(4)P affects Golgi particle movement we examined their trajectories in 3D using Sec7-GFP, as its apparent concentration was independent of PI(4)P levels (Fig. 4*A*). In both *pik1* cells in the absence of Dox and WT cells, a plot of Golgi particle average MSD vs. time revealed

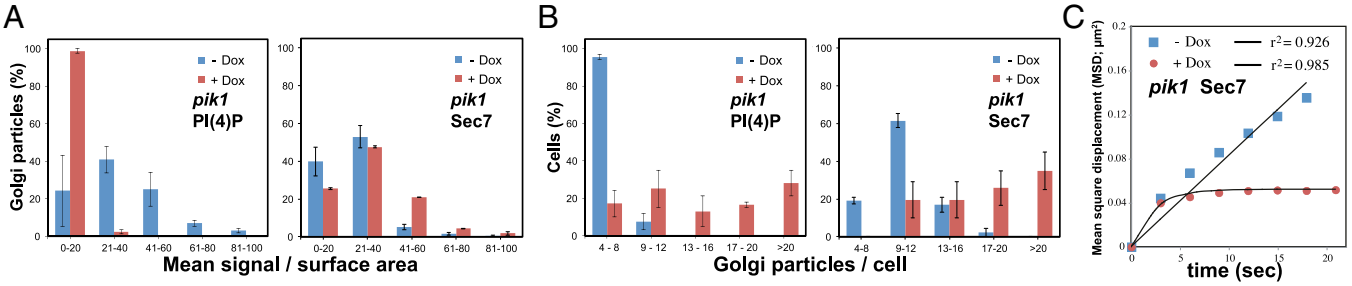

Fig. 4. Reduction of Golgi PI(4)P results in Golgi proliferation and confinement of movement. (*A*) Repression of *PIK1* results in a decrease in the effective Golgi PI(4)P concentration. The mean fluorescent signal and surface area of Golgi from 3D images were determined using Volocity. Shown are averages from two experiments ($n = 500–1{,}000$ Golgi particles analyzed, ∼50 cells); bars indicate average values from each experiment. (*B*) Reducing Golgi PI(4)P levels results in late Golgi proliferation. The number of Golgi particles per cell from strains as in *A* was determined using Volocity. (*C*) Golgi movement becomes confined upon reduction of Golgi PI(4)P. Multiple z sections were acquired every 2.8 s. Average MSD was from ∼400 Golgi tracks and data were fitted using QuanTrack according to Brownian or confined behavior. Similar results were observed in two independent experiments.

that the Golgi particles undergo random motion close to Brownian diffusion (Fig. 4*C* and Fig. S6*E*). Strikingly, upon reduction of the Golgi PI(4)P levels, movements were confined to an ∼0.6-μm diameter sphere (Fig. 4*C* and *SI Materials and Methods*). These analyses of Golgi movement did not reveal any directed movement, perhaps due to insufficient temporal resolution. Hence we examined movement in 2D, acquiring images every 0.35 s. Tracks were again separated based upon α and we observed a small number of tracks with directed Golgi movement in budding (2.4% of tracks) and hyphal cells (1.7% of tracks) (Fig. S4*F*). Together our results suggest that sufficient Golgi PI(4)P is critical for the unrestricted 3D Brownian movement of the bulk of the *C. albicans* Golgi.

Plasma Membrane PI(4)P Localizes as a Tight Cap at the Hyphal Tip. Our results suggest that Golgi PI(4)P is critical for the budding to hyphal transition and a previous study suggested that PM PI(4)P is also important for this transition (8). In *S. cerevisiae* the pools of PI(4)P at the Golgi and PM appear to be independent (9, 11), suggesting little Golgi PI(4)P reaches the PM. To determine whether Golgi PI(4)P contributes to the PM pool, we examined the distribution of PI(4)P. To visualize PM PI(4)P we used an Osh2 PH domain that specifically binds this lipid as a reporter, in which we mutated residues critical for Arf binding (32) (Fig. S7 *A* and *B*). As the high expression of this reporter perturbed cell growth, we used the *ACT1* promoter; the resulting strain grew identically to the WT. In WT cells we observed slightly more PI(4)P in small buds than in the mother cell (Fig. 5*A*). In contrast, a striking PI(4)P asymmetry was observed in germ tubes, irrespective of filament length and expression level of the reporter (Fig. 5*B* and Fig. S7*C*), and we quantified the total membrane signal from sum projections using the Matlab program HyphalPolarity (8).

To further characterize this PM PI(4)P distribution we modeled the spatiotemporal dynamics of PI(4)P in hyphal filaments. The levels of PI, PI(4)P, and PI(4,5)P_2 are interdependent (Eqs. **S1–S3** and *SI Materials and Methods*). Our model thus includes phosphorylation and dephosphorylation of PI, PI(4)P, and PI(4,5)P_2; lipid diffusion; lipid addition/removal via exocytosis/endocytosis; and dilution due to cell growth (Fig. 5*C* and *SI Materials and Methods*). We simplified this model by assuming that PI(4,5)P_2 → PI(4)P is negligible [PI(4)P distribution is unaffected in a *mss4* mutant] and that PI → PI(4)P and PI(4)P → PI(4,5)P_2 occur predominantly at the filament tip. Whereas Stt4 is uniformly distributed on the PM (8), PI is likely to be delivered to the tip via secretion (33) and Mss4 is localized at the tip (8). In this case, we can decouple the equation for PI(4)P from the others,

$$\partial_t p_1 = D\partial_{xx} p_1 - (\alpha_e + j_1) p_1, \qquad [1]$$

where p_1 is the concentration of PI(4)P; D is the PI(4)P membrane diffusion coefficient; α_e and j_1 are the rates of localized endocytosis and dephosphorylation; and PI transport to the tip via exocytosis, phosphorylation, i.e., PI → PI(4)P, PI(4)P → PI(4,5)P_2, and lipid dilution due to tip growth together determine the first boundary condition, i.e., the concentration of PI(4)P at the tip.

We have solved this equation in the quasi-steady state with a second boundary condition of no lipid flux at the base of the filament. We analyzed the solution with or without localized endocytosis, i.e., a 2-μm band of endocytosis (34, 35) revealed by a collar of Abp1-GFP 1–3 μm from the end of the filament, irrespective of length (Fig. 5*C* and Fig. S7 *C* and *D*) and with or without phosphatase-dependent hydrolysis of PI(4)P. The model predicts that this striking PI(4)P asymmetry is essentially dictated by phosphatase-dependent hydrolysis, with endocytosis playing a

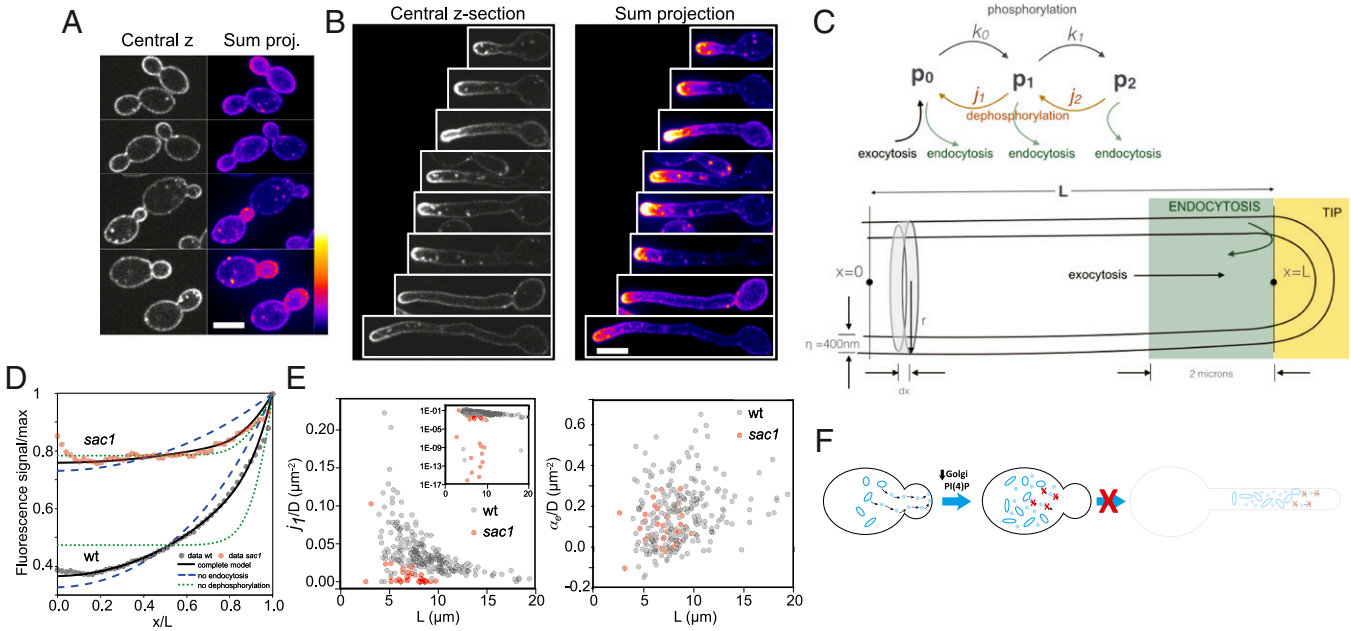

Fig. 5. Plasma membrane PI(4)P forms a tight cap at the hyphal filament tip. (*A*) PM PI(4)P is slightly enriched on small buds. Shown are central z sections and sum projections (false colored with LUT as shown) of WT cells expressing PI(4)P^{OSH2}. (*B*) PM PI(4)P localizes as a tight cap in hyphal cells. Cells as in *A* were incubated with FCS. (*C*) Schematic of modeling contributions of PI(4)P distribution in hyphal filaments. (*C*, *Upper*) Contributions to PI(4)P distribution, including phosphorylation/dephosphorylation and membrane traffic. (*C*, *Lower*) Schematic of analyses for PI(4)P distribution and regions of hyphal filament; x is distance from the cell body, r the filament radius, and dx the pixel length. The region in gray indicates an example of pixel volume, over which fluorescence is collected, green is where endocytosis occurs, and yellow is the tip region. L is the length of the filament where the PI(4)P concentration is fixed by the boundary condition. (*D*) The Sac1 phosphatase is critical for steep PM PI(4)P gradient. Average PM PI(4)P profiles from WT (gray) and *sac1* (red) hyphae are shown fitted with the solution to Eq. **1** with or without localized endocytosis (blue) or PI(4)P hydrolysis (green). Mean r^2 values for WT and *sac1* model fits: complete, 85% and 42%; no dephosphorylation, 55% and 33%; and no endocytosis, 72% and 3%. (*E*) PI(4)P dephosphorylation, but not endocytosis, is substantially reduced in the *sac1* mutant. Shown are PI(4)P dephosphorylation rate/D (*E*, *Left*) and endocytosis rate/D (*E*, *Right*) in WT (gray) and *sac1* (red) filaments in the complete model. (*F*) Scheme of the importance of Golgi PI(4)P for yeast to filamentous growth transition. Dark blue ovals (Golgi) and light blue circles (SVs) are indicated.

minor role (Fig. 5*D* and Fig. S8 *A* and *B*). Hence, we examined the PI(4)P distribution in hyphae lacking Sac1, the primary phosphatase responsible for regulating plasma membrane PI(4)P in *S. cerevisiae* (32, 36, 37). In this mutant there was a dramatic loss of the PI(4)P gradient (Fig. 5*D* and Fig. S8*C*); endocytosis is responsible for the residual PI(4)P asymmetry. Importantly, the rate of dephosphorylation is substantially reduced in *sac1*, whereas the endocytosis rate is unaffected (Fig. 5*E* and *SI Materials and Methods*). These models also predict that the dephosphorylation rate, but not that of endocytosis, correlates with the inverse of the length of the filament squared ($1/L^2$) (Fig. S8 *D–F*). The boundary condition critical for this distribution is the generation of PI(4)P at the filament tip.

Given that Stt4 is distributed uniformly along the filament PM (8), we assumed that delivery of PI via the secretory pathway promotes the generation of PI(4)P at the filament tip and the striking gradient. Consistent with the importance of actin-dependent secretion, disruption of the actin cytoskeleton with Latrunculin A, but not the septin cytoskeleton, resulted in a complete loss of PI(4)P asymmetry (Fig. S9 *A–C*). Golgi PI(4)P could also contribute to the PM pool of this lipid; however, PM PI(4)P was unaffected upon reduction of Golgi PI(4)P (Fig. S9*D*), suggesting that this is not the case. Conversely, there was no difference in the number of $PI(4)P^{FAPP1}$ Golgi per cell upon *STT4* repression (Fig. S9*E*); however, an increase of approximately twofold in the Golgi PI(4)P concentration was observed (Fig. S9*F*), suggesting that Stt4 may limit Golgi PI(4)P levels. Together, these results indicate that the two PI(4)P pools are distinct and that actin-dependent transport is critical for the PM PI(4)P distribution.

Discussion

Our results show that Golgi PI(4)P is critical for the *C. albicans* yeast to filamentous growth transition. Consistent with this, we show that Golgi PI(4)P is important for the distribution of PM proteins, that it is required for budding from the late Golgi and targeting of SVs to sites of growth, and that it is important for the unconstrained movement of these organelles. Concomitant with filamentous growth, we observed a tight cap of PM PI(4)P that was independent of filament length. Modeling of this steep PI(4)P gradient suggests that local delivery of PI to the filament tip and PI(4)P hydrolysis are critical for this distribution. Our results reveal that Golgi PI(4)P is important for the increased membrane traffic that is crucial for hyphal formation (Fig. 5*G*).

Golgi and Secretory Vesicle Dynamics. The distribution and dynamics of Golgi particles differ from those of SVs in both budding and filamentous cells. Fungi undergo hyphal growth at dramatically different rates (38, 39); for example, filament extension occurs >200-fold more rapidly in *N. crassa* than in *C. albicans*. Interestingly, Golgi particles are localized preferentially in the filament tip region in *C. albicans* and *Aspergillus nidulans* (15, 26, 40), but apparently not in *N. crassa* (41). Although directed Golgi movement is particularly difficult to detect in filamentous fungi, due to rapid 3D movement as well as saltatory movement (15, 40), it has been recently observed in *N. crassa* (41). In *C. albicans* a small fraction of SVs and Golgi particles exhibited directed movement in budding and filamentous cells. A substantial increase in SV MSD in hyphae (both for the $\alpha < 0.4$ and for the $\alpha > 1.4$ classes) was observed and as SVs moved more rapidly it was easier to observe directed movement in both cell types. It is interesting that 70–80% of particles, both SVs and Golgi, did not move in a directed fashion; i.e., $\alpha < 0.4$. Whereas single-plane acquisition underestimates directed vesicle movement, we observed the Golgi undergoing a jiggling-type movement and it is likely that these particles exhibit a combination of Brownian and directed movement perhaps indicative of maturation.

Golgi PI(4)P Function. Reducing Golgi PI(4)P levels results in defects in the Golgi and SVs that have functional consequences. In particular, a dramatic increase in the number of Golgi particles was observed, likely due to Golgi proliferation. The simplest explanation for this is that a defect in vesicle budding from the late Golgi results in a buildup of this compartment. Examination of the 3D Golgi dynamics revealed that the bulk of the Golgi movement is consistent with random Brownian diffusion; however, reduction of Golgi PI(4)P confined this movement to a sphere with a diameter of ~0.6 μm, indicating that PI(4)P at the Golgi is necessary for unrestricted movement. The actin cytoskeleton is critical for Golgi and SV movement in *A. nidulans* and *S. cerevisiae* (40, 42). As the actin cytoskeleton was largely unaffected in the *C. albicans pik1* mutant, we consider this scenario unlikely. Alternatively, we envision that Golgi PI(4)P may be important for the association of the Golgi particles to the myosin-V Myo2, as has been observed with *S. cerevisiae* SVs (11); indeed, recently PI(4)P has been shown to regulate a Golgi motor–cargo interaction (43). Reducing Golgi PI(4)P could lead to this organelle dissociating from myosin-V, resulting in an apparent confinement of movement. In striking contrast to what is observed in *S. cerevisiae* (11), there was little to no colocalization of PI(4)P with SVs in budding *C. albicans* cells [$1.8 \pm 1.2\%$ $PI(4)P^{FAPP1}$ colocalized with Sec4, $n > 2{,}000$ particles]. Further, the Golgi particles and SVs differed in their sizes, dynamics, MSDs, instantaneous velocities, and average α values. Indeed, even though we have been unable to generate strains with reduced Golgi PI(4)P in which we can follow Sec7 and Sec4, the distinct dynamics of Golgi particles and SVs argue against collapse or fusion of SVs into the Golgi.

Nonetheless, reduction of Golgi PI(4)P perturbs SV targeting, leading to a decrease in vesicles in small buds, as observed in *S. cerevisiae* (11, 22). The alterations in Golgi particle number and dynamics, as well as SV targeting, are likely responsible for the altered distribution of the multidrug transporter Cdr1 and the increased sensitivity to antifungal drugs. Furthermore, although we did not observe a defect in uptake of FM4-64 from the PM, its appearance at the vacuole was substantially delayed, most likely because this reporter passes through the late Golgi as in *S. cerevisiae* (44). We propose that these dramatic alterations in the late Golgi result in specific defects in the yeast to filamentous growth transition, as an increased level of membrane traffic is likely critical for hyphal formation. This is striking, as it has been previously shown that Sec3 is not required for this transition (45).

A Steep Plasma Membrane PI(4)P Gradient. Quantification of the distribution of PM PI(4)P in hyphal filaments revealed a steep gradient, in which the PI(4)P concentration decreased rapidly, moving away from the filament tip. We have generated a mathematical model, based on several simplifying assumptions, which accurately reproduces the PM PI(4)P distribution. This model predicts that the steep PI(4)P gradient is absolutely dependent on hydrolysis of PI(4)P by phosphatases, whereas endocytosis, which is not essential for filament formation (34, 35), fine-tunes the PI(4)P distribution. Indeed we observed a dramatic reduction in PI(4)P asymmetry in the *sac1* phosphatase mutant. Interestingly, the dephosphorylation rate inversely correlates with L^2 and equivalently λ_0 linearly correlates with L irrespective of endocytosis. We can envision a number of possibilities to explain this dependence, including nonlinear dephosphorylation kinetics, e.g., both the phosphatase and its regulator being diluted ($j_1 \propto J_1^2$).

This model highlights two major contributions to the PM PI(4)P distribution: hydrolysis by phosphatases and the restricted generation of PI(4)P at the filament tip, which is included in the boundary condition. The *C. albicans* genome contains several PI-phosphatases with a Sac1-like domain that can dephosphorylate PI(4)P, in particular Inp52 and Sac1 (there is no Inp53 homolog). In *S. cerevisiae* the former phosphatase is found in cortical actin patches (46) and the latter is found at the ER and Golgi (47) and is primarily responsible for regulating PI(4)P levels at the PM (32, 36) via Osh proteins at ER–PM contact sites (37). In *C. albicans* hyphal filaments Inp52 and Sac1 localized to cortical patches and to perinuclear and cortical ER, respectively, without an increased level at the back of the filament for either phosphatase. The low signals of these GFP phosphatase fusions precluded time-lapse experiments to determine whether their levels decreased as

filaments elongated. Our results indicate that the Golgi PI(4)P pools do not substantially contribute to the PM PI(4)P; however, as this *pik1* mutant does not form hyphal filaments, such analyses were only possible in budding *C. albicans*.

Membrane Traffic and Highly Polarized Growth. The morphological transition of *C. albicans* from budding to filamentous growth likely requires a substantial and sustained increase in membrane traffic to dramatically increase the PM and cell wall material necessary for generating a long filament. Tight regulation of membrane traffic, including the restricted location and distinct dynamics of organelles, e.g., the Golgi and exo/endocytic vesicles as well as the Spitzenkörper, is critical for the generation of highly elongated cells, including filamentous fungal hyphae and plant pollen tubes. The functionally separate pools of PI(4)P at the Golgi and PMs are crucial for fungal filamentous growth, in part due to their pivotal roles in membrane traffic, both for ensuring sufficient flux of membrane material and for its incorporation at the appropriate location. The multiple roles of PI(4)P in polarized growth are likely to be conserved in a range of organisms.

Materials and Methods

Strains and plasmids used and their construction are described in *SI Materials and Methods* and listed in Tables S1–S3.

Cells and colonies were imaged as described in ref. 39. Scanning confocal microscopy of fixed cells and spinning-disk confocal microscopy of all live cells were carried out as described in ref. 39. All Golgi images were deconvolved (Huygens Professional software; SN10). Unless indicated otherwise, error bars represent SD. Scale bar is 5 μm for cells and 1 mm for colonies.

Additional methods are included in *SI Materials and Methods*.

ACKNOWLEDGMENTS. We thank S. Bates, J. Berman, N. Dean, S. Emr, J. Konopka, J. Morschhäuser, J. Wendland, and Y. Wang for reagents; F. Besse, P. Follette, and M. Arkowitz for comments on the manuscript; and J. Thorner and E. Sartorel for their hospitality and stimulating discussions. We thank S. Bogliolo, M. Mondin, A. Vernay, and E. Goguet-Surmenian for assistance. This work was supported by the Centre National de la Recherche Scientifique and the Agence Nationale de la Recherche (ANR-13-BSV3-0006-01 and ANR-11-LABX-0028-01), Association pour la Recherche sur le Cancer (20141201949), France–Berkeley Fund (2012-0056), and European Union FP7 (PITN-GA-2013-607963) grants and the Platform of Resources in Imaging and Scientific Microscopy facility.

1. Strahl T, Thorner J (2007) Synthesis and function of membrane phosphoinositides in budding yeast, *Saccharomyces cerevisiae*. *Biochim Biophys Acta* 1771(3):353–404.
2. Santiago-Tirado FH, Bretscher A (2011) Membrane-trafficking sorting hubs: Cooperation between PI4P and small GTPases at the trans-Golgi network. *Trends Cell Biol* 21(9):515–525.
3. De Matteis MA, Wilson C, D'Angelo G (2013) Phosphatidylinositol-4-phosphate: The Golgi and beyond. *BioEssays* 35(7):612–622.
4. Flanagan CA, et al. (1993) Phosphatidylinositol 4-kinase: Gene structure and requirement for yeast cell viability. *Science* 262(5138):1444–1448.
5. Strahl T, Hama H, DeWald DB, Thorner J (2005) Yeast phosphatidylinositol 4-kinase, Pik1, has essential roles at the Golgi and in the nucleus. *J Cell Biol* 171(6):967–979.
6. Yoshida S, Ohya Y, Goebl M, Nakano A, Anraku Y (1994) A novel gene, *STT4*, encodes a phosphatidylinositol 4-kinase in the *PKC1* protein kinase pathway of *Saccharomyces cerevisiae*. *J Biol Chem* 269(2):1166–1172.
7. Garcia-Bustos JF, Marini F, Stevenson I, Frei C, Hall MN (1994) *PIK1*, an essential phosphatidylinositol 4-kinase associated with the yeast nucleus. *EMBO J* 13(10):2352–2361.
8. Vernay A, Schaub S, Guillas I, Bassilana M, Arkowitz RA (2012) A steep phosphoinositide bis-phosphate gradient forms during fungal filamentous growth. *J Cell Biol* 198(4):711–730.
9. Audhya A, Foti M, Emr SD (2000) Distinct roles for the yeast phosphatidylinositol 4-kinases, Stt4p and Pik1p, in secretion, cell growth, and organelle membrane dynamics. *Mol Biol Cell* 11(8):2673–2689.
10. Hama H, Schnieders EA, Thorner J, Takemoto JY, DeWald DB (1999) Direct involvement of phosphatidylinositol 4-phosphate in secretion in the yeast *Saccharomyces cerevisiae*. *J Biol Chem* 274(48):34294–34300.
11. Santiago-Tirado FH, Legesse-Miller A, Schott D, Bretscher A (2011) PI4P and Rab inputs collaborate in myosin-V-dependent transport of secretory compartments in yeast. *Dev Cell* 20(1):47–59.
12. Walch-Solimena C, Novick P (1999) The yeast phosphatidylinositol-4-OH kinase Pik1 regulates secretion at the Golgi. *Nat Cell Biol* 1(8):523–525.
13. Szentpetery Z, Várnai P, Balla T (2010) Acute manipulation of Golgi phosphoinositides to assess their importance in cellular trafficking and signaling. *Proc Natl Acad Sci USA* 107(18):8225–8230.
14. Matsuki T, et al. (2010) Reelin and stk25 have opposing roles in neuronal polarization and dendritic Golgi deployment. *Cell* 143(5):826–836.
15. Pantazopoulou A, Peñalva MA (2009) Organization and dynamics of the *Aspergillus nidulans* Golgi during apical extension and mitosis. *Mol Biol Cell* 20(20):4335–4347.
16. Kadosh D (2013) Shaping up for battle: Morphological control mechanisms in human fungal pathogens. *PLoS Pathog* 9(12):e1003795.
17. Sudbery PE (2011) Growth of *Candida albicans* hyphae. *Nat Rev Microbiol* 9(10):737–748.
18. Corvest V, Bogliolo S, Follette P, Arkowitz RA, Bassilana M (2013) Spatiotemporal regulation of Rho1 and Cdc42 activity during *Candida albicans* filamentous growth. *Mol Microbiol* 89(4):626–648.
19. Zhang X, et al. (2008) Membrane association and functional regulation of Sec3 by phospholipids and Cdc42. *J Cell Biol* 180(1):145–158.
20. Daboussi L, Costaguta G, Payne GS (2012) Phosphoinositide-mediated clathrin adaptor progression at the trans-Golgi network. *Nat Cell Biol* 14(3):239–248.
21. Lorente-Rodríguez A, Barlowe C (2011) Requirement for Golgi-localized PI(4)P in fusion of COPII vesicles with Golgi compartments. *Mol Biol Cell* 22(2):216–229.
22. Mizuno-Yamasaki E, Medkova M, Coleman J, Novick P (2010) Phosphatidylinositol 4-phosphate controls both membrane recruitment and a regulatory switch of the Rab GEF Sec2p. *Dev Cell* 18(5):828–840.
23. Prasad R, De Wergifosse P, Goffeau A, Balzi E (1995) Molecular cloning and characterization of a novel gene of *Candida albicans*, *CDR1*, conferring multiple resistance to drugs and antifungals. *Curr Genet* 27(4):320–329.
24. Sanglard D, Ischer F, Monod M, Bille J (1996) Susceptibilities of *Candida albicans* multidrug transporter mutants to various antifungal agents and other metabolic inhibitors. *Antimicrob Agents Chemother* 40(10):2300–2305.
25. Dowler S, et al. (2000) Identification of pleckstrin-homology-domain-containing proteins with novel phosphoinositide-binding specificities. *Biochem J* 351(Pt 1):19–31.
26. Rida PC, Nishikawa A, Won GY, Dean N (2006) Yeast-to-hyphal transition triggers formin-dependent Golgi localization to the growing tip in *Candida albicans*. *Mol Biol Cell* 17(10):4364–4378.
27. Godi A, et al. (2004) FAPPs control Golgi-to-cell-surface membrane traffic by binding to ARF and PtdIns(4)P. *Nat Cell Biol* 6(5):393–404.
28. He J, et al. (2011) Molecular basis of phosphatidylinositol 4-phosphate and ARF1 GTPase recognition by the FAPP1 pleckstrin homology (PH) domain. *J Biol Chem* 286(21):18650–18657.
29. Huang ZX, Wang H, Wang YM, Wang Y (2014) Novel mechanism coupling cyclic AMP-protein kinase A signaling and golgi trafficking via Gyp1 phosphorylation in polarized growth. *Eukaryot Cell* 13(12):1548–1556.
30. Losev E, et al. (2006) Golgi maturation visualized in living yeast. *Nature* 441(7096):1002–1006.
31. Franzusoff A, Redding K, Crosby J, Fuller RS, Schekman R (1991) Localization of components involved in protein transport and processing through the yeast Golgi apparatus. *J Cell Biol* 112(1):27–37.
32. Roy A, Levine TP (2004) Multiple pools of phosphatidylinositol 4-phosphate detected using the pleckstrin homology domain of Osh2p. *J Biol Chem* 279(43):44683–44689.
33. Yakir-Tamang L, Gerst JE (2009) A phosphatidylinositol-transfer protein and phosphatidylinositol-4-phosphate 5-kinase control Cdc42 to regulate the actin cytoskeleton and secretory pathway in yeast. *Mol Biol Cell* 20(15):3583–3597.
34. Caballero-Lima D, Kaneva IN, Watton SP, Sudbery PE, Craven CJ (2013) The spatial distribution of the exocyst and actin cortical patches is sufficient to organize hyphal tip growth. *Eukaryot Cell* 12(7):998–1008.
35. Zeng G, Wang YM, Wang Y (2012) Cdc28-Cln3 phosphorylation of Sla1 regulates actin patch dynamics in different modes of fungal growth. *Mol Biol Cell* 23(17):3485–3497.
36. Foti M, Audhya A, Emr SD (2001) Sac1 lipid phosphatase and Stt4 phosphatidylinositol 4-kinase regulate a pool of phosphatidylinositol 4-phosphate that functions in the control of the actin cytoskeleton and vacuole morphology. *Mol Biol Cell* 12(8):2396–2411.
37. Stefan CJ, et al. (2011) Osh proteins regulate phosphoinositide metabolism at ER-plasma membrane contact sites. *Cell* 144(3):389–401.
38. Hickey PC, Jacobson D, Read ND, Glass NL (2002) Live-cell imaging of vegetative hyphal fusion in *Neurospora crassa*. *Fungal Genet Biol* 37(1):109–119.
39. Bassilana M, Hopkins J, Arkowitz RA (2005) Regulation of the Cdc42/Cdc24 GTPase module during Candida albicans hyphal growth. *Eukaryot Cell* 4(3):588–603.
40. Hubbard MA, Kaminskyj SG (2008) Rapid tip-directed movement of Golgi equivalents in growing Aspergillus nidulans hyphae suggests a mechanism for delivery of growth-related materials. *Microbiology* 154(Pt 5):1544–1553.
41. Sanchez-Leon E, et al. (2015) The Rab GTPase YPT-1 associates with Golgi cisternae and Spitzenkorper microvesicles in *Neurospora crassa*. *Mol Microbiol* 95(3):472–490.
42. Rossanese OW, et al. (2001) A role for actin, Cdc1p, and Myo2p in the inheritance of late Golgi elements in *Saccharomyces cerevisiae*. *J Cell Biol* 153(1):47–62.
43. Niu Y, et al. (2013) PtdIns(4)P regulates retromer-motor interaction to facilitate dynein-cargo dissociation at the trans-Golgi network. *Nat Cell Biol* 15(4):417–429.
44. Bhave M, et al. (2014) Golgi enlargement in Arf-depleted yeast cells is due to altered dynamics of cisternal maturation. *J Cell Sci* 127(Pt 1):250–257.
45. Li CR, Lee RT, Wang YM, Zheng XD, Wang Y (2007) Candida albicans hyphal morphogenesis occurs in Sec3p-independent and Sec3p-dependent phases separated by septin ring formation. *J Cell Sci* 120(Pt 11):1898–1907.
46. Stefan CJ, Padilla SM, Audhya A, Emr SD (2005) The phosphoinositide phosphatase Sjl2 is recruited to cortical actin patches in the control of vesicle formation and fission during endocytosis. *Mol Cell Biol* 25(8):2910–2923.
47. Whitters EA, Cleves AE, McGee TP, Skinner HB, Bankaitis VA (1993) SAC1p is an integral membrane protein that influences the cellular requirement for phospholipid transfer protein function and inositol in yeast. *J Cell Biol* 122(1):79–94.